

0.2

RECEIVED
LAWRENCE
RADIATION LABORATORY

DEC 1 1970

LIBRARY AND
DOCUMENTS SECTION

MOLECULAR-BEAM KINETICS. II.
MAGNETIC DEFLECTION ANALYSIS OF REACTIONS
OF Li WITH NO₂, CH₃NO₂, SF₆, CCl₄, AND CH₃I

David D. Parrish and Ronald R. Herm

October 1970

AEC Contract No. W-7405-eng-48

TWO-WEEK LOAN COPY

*This is a Library Circulating Copy
which may be borrowed for two weeks.
For a personal retention copy, call
Tech. Info. Division, Ext. 5545*

UCRL

LAWRENCE RADIATION LABORATORY
UNIVERSITY of CALIFORNIA BERKELEY

UCRL-20356

34

0.2

DISCLAIMER

This document was prepared as an account of work sponsored by the United States Government. While this document is believed to contain correct information, neither the United States Government nor any agency thereof, nor the Regents of the University of California, nor any of their employees, makes any warranty, express or implied, or assumes any legal responsibility for the accuracy, completeness, or usefulness of any information, apparatus, product, or process disclosed, or represents that its use would not infringe privately owned rights. Reference herein to any specific commercial product, process, or service by its trade name, trademark, manufacturer, or otherwise, does not necessarily constitute or imply its endorsement, recommendation, or favoring by the United States Government or any agency thereof, or the Regents of the University of California. The views and opinions of authors expressed herein do not necessarily state or reflect those of the United States Government or any agency thereof or the Regents of the University of California.

MOLECULAR-BEAM KINETICS. II.

MAGNETIC DEFLECTION ANALYSIS OF REACTIONS
OF Li WITH NO₂, CH₃NO₂, SF₆, CCl₄, AND CH₃I

David D. Parrish* and Ronald R. Herm†

Inorganic Materials Research Division,
Lawrence Radiation Laboratory and
Department of Chemistry, University of California
Berkeley, California 94720

ABSTRACT

Thermal energy crossed molecular beam studies have been made of the reactions of Li with NO₂, CH₃NO₂, SF₆, CCl₄, and CH₃I. An inhomogeneous deflecting magnet between the collision zone and detector was used to distinguish elastic scattering of Li from reactive scattering of LiZ. The total reaction cross sections and the reactive attenuations of the wide-angle Li non-reactive scattering for these gases are considerably smaller than are the corresponding features previously reported for the

* Present address: Department of Chemistry, Harvard University,
Cambridge, Massachusetts.

† Alfred P. Sloan Foundation Fellow.

Li + XY (XY = Cl₂, Br₂ and ClI) reactions. Interesting differences are observed in the LiZ center-of-mass (CM) product angular distributions for the five gases studied here. The LiO product of the NO₂ reaction is more sharply forward peaked in the direction of the incoming Li atom than are the corresponding LiX products of the Li + XY reactions. The LiNO₂ and LiF products of the CH₃NO₂ and SF₆ reactions exhibit very broad, almost isotropic CM angular distributions. The LiCl and LiI products of the CCl₄ and CH₃I reactions are predominantly scattered into the backward hemisphere in the CM coordinate system. The features of the NO₂ reaction are discussed in terms of the electron transfer mechanism which was originally advanced to account for the features of the reactions of the alkali atoms with the halogen molecules.

This paper describes a continuing¹ crossed molecular beam study of Li atom reactions and presents results obtained from angular distribution measurements for the reactions of Li with NO_2 , CH_3NO_2 , SF_6 , CCl_4 , and CH_3I . Part I of this series¹ reported results for the reactions of Li with the halogen molecules (and with two polyhalogenated molecules as well). These reactions of the alkali atoms (M) with halogen molecules (XY) are characterized by scattering of the alkali halide (MX) products predominately into the forward hemisphere in the center-of-mass (CM) coordinate system (i.e., the A + BC reaction is defined as forward scattered if the AB product is scattered predominately in the direction of the incoming A particle); this behavior has been phenomenologically termed "stripping." Part I disclosed interesting similarities and differences between the features of the reactions of halogen molecules with Li and with the heavier alkali atoms. The aim of the present study is to further contrast the behavior of Li and the heavier alkali atoms by studying the reactions of Li with five reactants which have been found to span a wide range of chemical behavior in their reactions with the heavier alkali atoms.

Studies of the K, Rb, and Cs + CH_3I reactions yielded the first measurements of product angular distributions from crossed molecular beams² and indeed proved to be prototype examples of a so-called "rebound" reaction where the product MX rebounds opposite to the direction of the incoming M

reactant. A later study³ indicated similar characteristics for the Na + CH₃I reaction. The Cs + CCl₄ reaction was probably the first chemical reaction of neutral species to be observed in a molecular beam experiment.⁴ Crossed beam product angular distribution measurements of the K, Rb, and Cs + CCl₄ reactions⁵ indicated that these reactions were intermediate in behavior between the "rebound" and "stripping" limits; moreover, product velocity analysis data⁶ indicated that these were the first reactions of neutral species to exhibit strong coupling between the product angular and translational recoil energy distributions. A series of investigations of the Cs + SF₆ reaction⁷ have recently shown that the product CsF translational, rotational, and vibrational energy distributions as well as the angular distribution are all consistent with a long-lived collision complex reaction model; the diversity of the methods employed and the quality of the results obtained establish this system as one of the most completely investigated chemical reactions. A previous crossed beam study of the K + CH₃NO₂ reaction⁸ indicated a very broad KNO₂ product angular distribution.

A recent investigation⁸ has yielded a limited amount of information concerning the characteristics of the reactive scattering of the four heavier alkali atoms from NO₂, but the present work represents the first measurement of a product angular distribution. Ref. 8 further pointed out that the high electron affinity⁹ of NO₂ suggests interesting parallels and contrasts between the reactions of the alkali atoms with the halogen molecules and with NO₂. Consequently the NO₂ reaction was studied here because it promised to be especially interesting as a test of the electron transfer mechanism originally advanced to account for the features of the reactions of the alkali atoms with the halogen molecules.

EXPERIMENTAL CONDITIONS

Only a brief description of the apparatus and experimental procedures will be given here; details are included in Part I and are described more extensively in Ref. 10. The two beams were crossed at an angle of 90° with their full thermal velocity distributions. The Li beam was prepared by thermal effusion from a conventional two-chamber oven source with standard knife-edge slits; the Li_2 concentration in the beam was negligible. The reactant gas was prepared on an external line at the desired pressure and emerged from a variable temperature, "crinkly foil" many channel source.

The angular distributions of scattered Li and LiZ were measured by surface ionization on a continuously oxygenated W filament; only scattering in the plane of the reactant beams was measured. Arguments presented in Part I indicate that this W surface ionized Li and LiX with very nearly equal efficiencies. When energized, an inhomogenous electromagnet placed between the collision zone and detector deflected aside a known fraction of the Li atoms, thereby providing a measure of the scattered Li and LiZ separately.

Correction has been made for the fact that the measured angular distributions were distorted by the angle dependent fraction of the collision zone seen by the detector through the collimating slits of the magnet (the viewing factor correction procedure is discussed in Part I); the experimentally determined correction factor was in all cases in satisfactory agreement with that calculated from the slit geometry. Each scattered signal is plotted as a relative intensity, a dimensionless quantity which is defined as the measured scattered intensity divided by the attenuation of the Li beam produced by the cross beam. Experiments were always run at a relative

Li beam attenuation of less than 10%. The measured laboratory (LAB) angular distributions are shown in Fig. 1.

RESULTS AND KINEMATIC ANALYSIS

Elastic Scattering

Figure 2 shows the center-of-mass (CM) elastic scattering of Li atoms obtained by transforming the LAB angular distributions by the conventional procedure¹¹ of assigning to the two scattering partners their most probable source velocities and assuming that all non-reactive scattering was due to elastic collisions. As Fig. 2 indicates, the two CM branches do give the same intensity, except at points obtained by transforming wide negative LAB angles where the approximate transformation procedure employed is known to be especially bad. With the exception of the NO₂ case, the wide-angle Li elastic scattering produced by the reactive gases is less than that produced by cyclohexane when the narrow-angle elastic scattering of the reactive gases are normalized to that of cyclohexane. This attenuation of the elastic scattering is a well known phenomenon and is generally interpreted as a depletion of the Li scattering due to reaction¹². However, the reactive attenuations shown in Fig. 2 are appreciably less than those reported in Part I for the reaction of Li with halogen molecules. A particularly interesting feature is that NO₂ apparently produces more very wide-angle Li scattering than does cyclohexane. This would be the expected behavior if a sufficient fraction of the non-reactive scattering of Li from NO₂ proceeded via formation of an intermediate complex with a lifetime long compared to its rotational periods. Indeed, the non-reactive scattering of alkali atoms from related oxides (notably SO₂) is known¹³ to proceed via this long-lived complex mechanism. The Li + NO₂ data shown in

Fig. 2 is suggestive of this mechanism, but a final decision must await experiments with a velocity selected Li beam.

Reactive Scattering

Figures 3-7 show the LAB angular distributions of the halide, oxide, and nitrite products. The error bars indicate only the uncertainty introduced by errors in the determination of the transmission of the Li atoms through the magnetic field; as discussed in Part I, this is the primary source of error near the Li beam but other inaccuracies certainly dominate at wide angles. Also shown are kinematic diagrams indicating LiZ recoil velocities for some of the possible final relative translational product recoil energies, E' . The total energy available to the products must be partitioned between E' and internal excitation W' and is given by

$$E' + W' = E + W + \Delta D_0,$$

where $E = \frac{1}{2} \mu V^2$ is the initial relative kinetic energy, W is the initial thermal internal excitation of the reactant, and ΔD_0 is the difference in LiX and R-X bond dissociation energies.

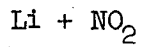
Figures 3-7 also show the calculated¹⁴ distributions in centroid angles, for an energy independent collision cross section, resulting from the thermal velocity distributions in both beams. These figures indicate that for NO_2 most of the product appears in the LAB to the left of the centroid distribution; for CH_3I and CCl_4 the product is scattered predominantly into angles to the right of the centroid distributions; whereas CH_3NO_2 and SF_6 produce appreciable product intensities at angles both to the right and to the left of the calculated centroid distributions. These qualitative observations indicate that: the Li + NO_2 product predominantly scatters into the forward hemisphere in the CM system (i.e., in the same

direction as that of the attacking Li atoms); $\text{Li} + \text{CH}_3\text{I}$ and CCl_4 predominantly scatter products into the backward CM hemisphere; while $\text{Li} + \text{SF}_6$ and CH_3NO_2 must produce very broad CM product angular distributions.

The LAB product angular distributions were transformed into the CM coordinate system by the same fixed velocity approximation (FVA) procedure used to transform the elastic scattering. Here again the reactants were assumed to have their most probable source velocities. However, owing to the distribution of final translational energy as well as scattering angle for the reaction products, two additional approximations were required: (1) that the angular and E' distributions were independent; and (2) that the E' distribution could be approximated by a delta function. The product LAB distributions were transformed for different assumed values of E' until positive and negative CM scattering angles gave a consistent CM angular distribution. Extensive computer studies¹⁵ have indicated that the CM angular distributions obtained from the FVA procedure are usually reliable, although somewhat broader than the true distributions. The values of E' derived may be relatively inaccurate (somewhat too low), although they do provide a qualitative indication of the energy partitioning.

Table I lists the values of the product recoil energies which provided the best FVA-CM product angular distributions; also listed are the ranges of E' values for each reaction which provided satisfactorily consistent FVA-CM product angular distributions. Table II gives the coefficients of an expansion of the derived LiZ -CM product angular distributions given in Figs. 8 and 9 in terms of the Legendre polynomials. As a partial check of these derived CM- LiZ distributions, they were used to back-calculate the LAB distributions by holding E' fixed and averaging over the thermal velocity distributions in both beams. Owing to the different chemical behaviors

of the five scattering gases studied here, separate discussions of the FVA derived CM distributions and back-calculated LAB distributions are given below.



The reaction of Li with NO_2 almost certainly produces LiO product, i.e.,



thermochemical arguments advanced in Ref. 8 eliminate the possibility of LiN or LiNO as the product of the reaction. The possibility of a LiNO_2 product which could be formed from N_2O_4 in the NO_2 beam was precluded by maintaining conditions in the reactant NO_2 beam such that only a negligible amount of the dimer could be present.¹⁶

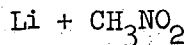
Since this present experiment employed magnetic deflection analysis to experimentally distinguish the non-reactive and reactive scattering, the angular distributions reported in Figs. 1,2,3, and 8 for the scattering of Li from NO_2 were arrived at by assuming that the product LiO was diamagnetic. In view of the fact that LiO has an unpaired electron, this assumption deserves close scrutiny. The LiO molecule is known to have a $^2\pi$ ground state.¹⁷ Since the interaction of the electron spin with the external field would be $\sim 0.7 \text{ cm}^{-1}$ (for a field of $\sim 15 \text{ kG}$), the spin-orbit intramolecular interaction is probably considerably greater than the interaction of either spin or orbital angular momentum with the external field. Under these conditions, the spin angular momentum would be coupled to the internuclear axis via the orbital angular momentum provided that the rotational excitation was insufficient to uncouple the spin; Hund's coupling case (a)¹⁸ would then be applicable. The $^2\pi_{1/2}$ state would have no magnetic dipole moment while the $^2\pi_{3/2}$ state would have a magnetic dipole that would be

rotationally averaged to near zero. This averaging is not complete, however. For example, a total angular momentum of $\sim 15\hbar$ would lead to an absolute value of the time averaged component of the magnetic moment in the field direction, averaged over all M_J states, of approximately 10% of the Bohr magneton, μ_0 ; some M_J states would have effective magnetic dipoles of up to $0.05 \mu_0$ for total angular momentum as high as $60\hbar$. Since a rotational excitation of 2 kcal/mole in the LiO (the approximate rotational excitation of KBr from $K + Br_2$ ¹⁹) corresponds to approximately $23\hbar$ and an upper limit of about $56\hbar$ is imposed by energy conservation, at least a small fraction of the LiO product is expected to be deflected aside in this experiment if Hund's coupling case (a) is applicable. Two possible further complications must be considered. First the spin may become uncoupled from the internuclear axis at high rotational excitation. Under complete uncoupling, Hund's coupling case (b)¹⁸ would apply, indicating a distribution of time averaged effective magnetic moments from $-\mu_0$ to $+\mu_0$ (depending on the M_J state) for the $^2\pi$ state. Secondly, although LiO is known to have a $^2\pi$ ground state, KO and CsO apparently have $^2\Sigma$ ground states⁸. This suggests that perhaps LiO has a low lying $^2\Sigma$ excited state (which would behave as paramagnetic Li; see Ref. 8 or 18) that could be appreciably populated in the reaction; ab initio calculations do indicate a $^2\Sigma$ excited state of LiO about 9 kcal/mole above the $^2\pi$ ground state²⁰. Both of these effects would of course increase the fraction of the LiO deflected by the magnet and thus be interpreted as non-reactive Li scattering rather than reactive LiO scattering.

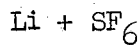
The rotational excitation in the alkali halide products of a number of alkali atom reactions have now been measured¹⁹ and in no case has there been any observable coupling between the angle of deflection and the

rotational energy distribution; therefore one may reasonably expect that there would be no strong coupling in this reactive system either. Since any $^2\Sigma$ product would be virtually completely deflected and, in the absence of a dependence of the LiO rotational excitation on scattering angle, the fractional deflection of the $^2\Pi$ product would be independent of scattering angle, Figs. 3 and 8 give the shapes of the angular distributions of only the $^2\Pi$ ground state LiO product. However, owing to the possibility that a significant fraction of the LiO might be deflected aside by the analyzing magnet, Fig. 2 gives an upper limit to the elastic scattering of Li from NO_2 and the $\text{Li} + \text{NO}_2$ total reactive cross reaction derived in a later reaction is a lower limit. An apparatus is currently being assembled which will allow velocity as well as magnetic deflection analysis of scattered species. Whereas the apparatus employed here only distinguished "diamagnetic" from "paramagnetic" Li species, this improved apparatus should provide a rough value for the magnetic dipole moment of the scattered species and should thus resolve uncertainties in this work concerning the magnetic behavior of LiO.

The LiO LAB distribution shown in Fig. 3 was transformed into the CM system by the FVA procedure. Consistent CM angular distributions were obtained for E' in the range of 2 to 3 kcal/mole; the angular distribution shown in Fig. 8 refers to $E' = 2.4$ kcal/mole, but the shape of the angular distribution changed only slightly as E' was varied from 2 to 3 kcal/mole. The LAB angular distribution back-calculated by averaging over the thermal velocity distributions in both beams with $E' = 2.4$ kcal/mole is shown in Fig. 3; here again, back-calculations for E' in the ranges 2-3 kcal/mole gave similar agreements with the original LAB distribution.

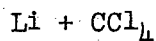


The magnetic deflection analysis presented in Ref. 8 and an electric deflection investigation reported in Ref. 19b indicate that the major products of the reactions of K and Cs with CH_3NO_2 are the corresponding alkali nitrites; by extrapolation, we expect the product from the present reaction to be LiNO_2 . However, the formation of the alkali oxide (MO) is probably also an exoergic reaction channel for all three reactions and is almost certainly the most exoergic for the Li reaction, although formation of MNO_2 is certainly favored energetically over formation of MO for all these reactions. Future electric deflection experiments should be able to determine if there is any LiO contribution to the reactive scattering; all analysis and discussion here assumes only LiNO_2 product. The CM distribution shown in Fig. 9 obtained by FVA transformation with $E' = 10.4$ kcal/mole is very similar to the consistent CM angular distributions provided by FVA for E' in the range 9-11 kcal/mole. Figure 4 shows the back calculated LAB distribution with $E' = 10.4$ kcal/mole.



The derivation of the CM angular distribution by the FVA procedure and the back-calculation were performed with $E' = 1.6$ kcal/mole; once again, consistent CM angular distributions were obtained for a range of E' , 1-2 kcal/mole; and these angular distributions were very similar to that shown in Fig. 9. In addition a symmetric distribution (dash-dot-dash curve in Fig. 9) was obtained by reflecting the FVA derived distribution for $\theta < 90^\circ$ through $\theta = 90^\circ$; back-calculation with this symmetric curve is also shown in Fig. 5 and is seen to fit the LAB data well except at large positive LAB

scattering angles ($\theta \gtrsim 100^\circ$). Thus, the data clearly indicate a broad CM-LiF product angular distribution with a peak in the forward direction at $\theta = 0^\circ$. The indications are that the product angular distribution is probably not symmetric about $\theta = 90^\circ$, although this conclusion must be regarded as very tentative pending product velocity analysis experiments, owing to the poor quality of the data at these large LAB scattering angles and to the approximate transformation procedures employed.



Recent product velocity analysis experiments on the reactions of the heavier alkali metals with CCl_4 have indicated⁶ that the E' distribution varies markedly with scattering angle for these reactions. Consequently, the FVA transformation procedure is expected to be an especially bad technique in the case of $\text{Li} + \text{CCl}_4$. Nevertheless, the FVA derived LiCl-CM angular distribution for $E' = 17$ kcal/mole is shown in Fig. 9 to give a qualitative indication of the product angular distribution, and is compared with approximate product angular distributions for reactions of the heavier alkali metals taken from Ref. 5. The FVA transformation of the data of Fig. 6 yields consistent CM angular distributions for a range of E' values from 1 to 40 kcal/mole. The qualitative shape of the CM angular distribution obtained is independent of the E' value taken, although the location of the peak does vary from $\theta = 120^\circ$ to 110° to 100° as E' is varied from 1 to 2 to 25 kcal/mole respectively. Figure 6 shows the back calculation at $E' = 17$ kcal/mole for the solid curve of Fig. 9; the dash-dot-dash curve extended flat to 180° from the peak of the solid curve of Fig. 9 was used with $E' = 2$ kcal/mole to back-calculate the dash-dot-dash curve of Fig. 6. These two curves demonstrate the almost complete lack of sensitivity of the

measured LAB distribution to the form of the CM angular distribution for CM scattering angles larger than the angle at which $I_{\text{LiCl}}(\theta)$ peaks. However, back-calculations with a CM angular distribution symmetric about $\theta = 90^\circ$ (i.e., translate the solid curve of Fig. 9 by -10° and reflect $\theta < 90^\circ$ through $\theta = 90^\circ$) do not reproduce the LAB distribution for any value of E' , indicating that the reaction must scatter products predominately into the backward CM hemisphere.

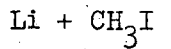


Figure 9 shows the FVA derived LiI-CM product distribution for $E' = 15$ kcal/mole. The FVA transformation provided consistent CM distributions (similar to that shown in Fig. 9) for E' in the range 12 - 20 kcal/mole. The FVA transformation also provided a consistent CM distribution for a second, lower range to E' values; in this energy range, the LAB \rightarrow CM transformation was double valued and the fit was rejected because back-calculations failed to reproduce the LAB distribution at negative values of θ . Figure 7 shows back-calculations for $E' = 15$ kcal/mole of both of the LiI-CM angular distributions shown in Fig. 9. The FVA derived CM distribution provided an adequate fit to the measured LAB distribution for E' in the range 15-20 kcal/mole; back-calculations with the CM distribution flat from $\theta = 120^\circ$ to 180° adequately fit the LAB distribution for E' in the range 10-15 kcal/mole, indicative again of the lack of sensitivity of the measured LAB distribution to the very wide-angle CM distribution.

Total Reaction Cross Sections

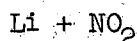
Table III gives values of the total reaction cross sections calculated by the two methods described in Part I ($Q_R(A)$ and $Q_R(B)$ calculated by

methods A and B respectively). Also listed are the estimated van der Waal's coefficients, C , for the interaction of the two gases, the calculated total collision cross sections, $Q_{t,abs}$, and calculated resolution corrected total collision cross sections $Q_{t,abs}^{eff}$. The reactive cross sections were calculated assuming equal Li and LiZ ionization efficiencies (this assumption is discussed in Part I); the geometric parameters required for the calculations were the same as those reported in Part I. The force constants, C , were calculated from the Slater-Kirkwood approximation with 1, 17, 24, 48, 32, and 14 effective numbers of electrons for Li, NO_2 , CH_3NO_2 , SF_6 , CCl_4 , and CH_3I . The polarizability values used were (in Å^3): 20 for Li;²¹ 3.1 for NO_2 ;²² 7.2 for CH_3NO_2 ;²³ 6.2 for SF_6 ;²³ 11.1 for CCl_4 ;²³ and 8.0 for CH_3I .²³ The induction terms were calculated using dipole moments of 0.29, 3.1, and 1.65 Debyes²⁴ for NO_2 , CH_3NO_2 , and CH_3I respectively.

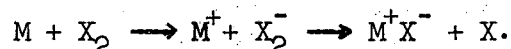
As may be seen in Fig. 2, the shapes of the narrow-angle CM elastic scattering angular distribution for these reactions exhibited significant deviations from one another, from that for the elastic scattering of Li from cyclohexane, and from the theoretically predicted small-angle elastic scattering form factor, $F(\theta, \theta_R)$, derived in Part I; these deviations were especially pronounced for the scattering of Li from NO_2 and SF_6 . While probably an experimental artifact, these deviations introduce additional ambiguities into the normalization of the small-angle elastic scattering to $F(\theta, \theta_R)$. This in turn introduces additional uncertainties in the total reactive cross section values deduced by Method A. However, the very good agreement between $Q_R(A)$ and $Q_R(B)$ values shown in Table III would suggest that any errors introduced by this effect were small. Other probable sources of error in the calculated total reactive cross sections are discussed in Part I. In general, the quoted total reaction cross sections are estimated to be closer than a factor of two to the true values. Moreover, the ratio

of derived Q_R values for any two gases is expected to be somewhat more accurate than are the individual values.

DISCUSSION



This reaction appeared likely to be of special interest for comparison with the alkali atom-halogen molecule reactions which are strongly exothermic and are believed²⁵ to proceed by a long-range electron transfer followed by almost immediate separation of the products,



The electron transfer occurs at the distance of separation, R_c , where, neglecting the ion-induced dipole forces, the Coulombic potential energy is equal to the difference between the ionization potential of M, $I(\text{M})$, and the vertical electron affinity of X_2 , $E_v(\text{X}_2)$:

$$e^2/R_c = I(\text{M}) - E_v(\text{X}_2). \quad (1)$$

The electron affinity of NO_2 is high,⁹ probably higher than that of the diatomic halogen molecules, but the electron affinity of O is much less than that of a halogen atom. Thus, the $\text{Li} + \text{NO}_2$ reaction is much less exoergic than the $\text{M} + \text{X}_2$ reactions; whereas the electron transfer can take place at large separation of the reactants, the $\text{Li}^+ - \text{NO}_2^-$ ion pair formed must approach to within much closer distances before the LiO and NO products can begin to separate. The potential energy surface for this reaction is therefore expected to exhibit relatively restricted entrance and exit channels with a deep chemical well corresponding to the formation of the strongly bound LiNO_2 intermediate. On the other hand, the expected potential energy surfaces for alkali atom-halogen molecule reactions exhibit no appreciable well and a wide exit channel.²⁶

These features of the potential energy surface of the $\text{Li} + \text{NO}_2$ system might have been expected to favor a reaction which proceeded via formation of an intermediate, long-lived complex. However, the observed sharp forward peaking of the LiO product is characteristic of the ultra-direct mechanism found for the $\text{M} + \text{X}_2$ reactions and indicates that the reaction is complete in a time shorter than the rotational period of the complex. The observation of such similar product distributions for both the $\text{Li} + \text{NO}_2$ reaction and the alkali metal+diatomic molecule reactions provides further evidence that the mechanism of the $\text{M} + \text{X}_2$ reactions is more involved than a simple "spectator stripping" behavior.

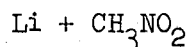
The sharp forward product peaking observed here has previously been characteristic of reactions with very large total reaction cross sections so that most of the reactive events corresponded to collisions with relatively large impact parameters. The $\text{Li} + \text{NO}_2$ total reaction cross section observed here (15 \AA^2) is in striking contrast to the much larger reaction cross sections reported in Part I for the $\text{Li} + \text{X}_2$ reactions (e.g., $Q_R = 85 \text{ \AA}^2$ for $\text{Li} + \text{Cl}_2$). The high electron affinity of NO_2 would predict a crossing of the covalent and ionic potential curves at large $\text{Li}-\text{NO}_2$ separations; values of 4.3 and 10 \AA for R_c and of 60 and 310 \AA^2 for Q_R would be calculated by Eq. (1) for NO_2 electron affinities of 45 and 90 kcal/mole respectively. Thus, even the lowest estimate of $E_v(\text{NO}_2)$ (45 kcal/mole; Ref. 8) would predict a total reaction cross section four times larger than that observed here. Owing to the unpaired spins of both Li and NO_2 , however, the quantum number for total spin of the collision partners may be 1 or 0. Moreover, the potential energy curve for ground state ions has zero total spin and so can interact only with the spin singlet potential energy surface for the neutral $\text{Li} + \text{NO}_2$ collision. If the neutral spin triplet potential energy

surface produced solely non-reactive scattering, the measured total reaction cross section would be 25% of that which would be predicted by Eq. (1) neglecting considerations of total spin. This would bring the measured total reaction cross section into agreement with the lowest estimates provided by the electron transfer mechanism. However, the most recent estimate²⁷ of $E_v(\text{NO}_2)$ suggests that it is probably higher than 83 kcal/mole so that R_c is expected to be closer to the 10 Å than to the 4.3 Å limit estimated from Eq. (1). If the covalent-ionic ground state crossing distance is indeed this large, the incoming Li atom might not be able to transfer the electron efficiently over such a distance.^{8,25} Under these conditions, the actual crossing distance would be computed from Eq. (1) by using an electron affinity for an excited state of NO_2^- . This would of course have the effect of reducing R_c . Since NO_2 is expected to exhibit excited triplet as well as singlet states, this would have the effect of enabling all of the Li- NO_2 trajectories reaching small enough internuclear distances to participate in the electron transfer mechanism and a Q_R value considerably in excess of that measured would still be expected. Alternatively, some of the collision events which cross over to the ionic surfaces might produce non-reactive scattering or the production of LiO in a $^2\Sigma$ state or a $^2\Pi$ state which is deflected aside by the magnet might account for the possible discrepancy between the measured Q_R and the predictions of Eq. (1).

These $M + \text{NO}_2$ reactions are also of special interest for comparison with a spectator stripping model²⁸ which gives the total reaction cross section approximately as $Q_R = \pi R_s^2$ with R_s equal to a critical distance for reactant approach computed by equating the Coulombic potential energy of product MO formation to the energy required to sever the O-NO bond,

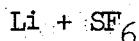
$$e^2/R_s = I(M) - E(O) + D_o(\text{O-NO}). \quad (2)$$

Here $E(0)$ is the electron affinity of the oxygen atom, 34 kcal/mole ,²⁹ and R_s and Q_R are calculated by Eq. (2) as 2.1 \AA and 13 \AA^2 respectively. This is in surprisingly good agreement with the experimental value of Q_R , but cannot be taken as evidence in favor of Eq. (2) and the spectator stripping model over the electron jump model (Eq. (1)) until the ambiguities associated with the possible production of a paramagnetic LiO species are resolved. For most of the reactions previously studied, R_c was similar to R_s or else uncertainties regarding the electron affinity of the parent species precluded a definitive test between these two models. An exception to this was however provided by the study of the reactions of Rb and Cs with NOCl where R_c is calculated to be much smaller than R_s ; for these reactions, the experimentally measured³⁰ reaction cross sections favor the electron jump model, Eq. (1), over Eq. (2) and the spectator stripping model.



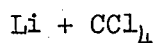
This reaction bears many resemblances to the $\text{Li} + \text{CH}_3\text{I}$ reaction. In both cases, a reactive group is abstracted from a methyl radical by the attacking Li atom and the product is formed with a high translational energy. Moreover, the strengths³¹ of the $\text{CH}_3\text{-I}$ and the $\text{CH}_3\text{-NO}_2$ bonds are virtually identical. Although the Li-NO_2 bond strength is unknown, it seems likely⁸ that it is comparable to that of an alkali halide so that the reaction exoergicities are similar for these reactions. Moreover, Table III indicates that the long range van der Waals interactions between the reactants are quite similar for the two cases. The enhanced CH_3NO_2 reaction cross section shown in Table III might simply be a consequence of the larger geometric size of the NO_2 group relative to that of an I atom. Trajectory calculation studies³² have shown that for a direct reaction proceeding without formation of an intermediate long-lived complex,

the product angular distribution could change from a strong anisotropic backward peaking to an isotropic CM distribution as the total reaction cross section is increased. This prediction is in qualitative accord with the trend observed here, although these same trajectory calculation did not report an even further change to forward product scattering (as is observed here for CH_3NO_2) as Q_R was further increased. Alternately, as discussed in connection with the $\text{Li} + \text{SF}_6$ reaction in the next section, the very broad product angular distribution shown in Fig. 9 might indicate that the reaction proceeds via formation of a complex with a lifetime comparable to its rotational period.

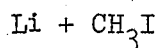


The total reaction cross section given in Table III correlates nicely with the values derived from the attenuation of the elastic scattering of K from SF_6 reported in Ref. 33 ($Q_R(K) \sim 21 - 50 \text{ \AA}^2$). As mentioned in the introduction, the reported⁷ CsF angular distribution and vibrational, rotational, and translational recoil energy distributions indicate that the $\text{Cs} + \text{SF}_6$ reaction proceeds via formation of an intermediate complex long-lived relative to a rotational period of the complex. An intermediate long-lived LiSF_6 complex would be expected to approximate a prolate top with three similar rotation constants. Formation of such an intermediate complex would, according to the statistical complex model³⁴, produce a broad symmetric CM-LiF product angular distribution peaking at $\theta = 0^\circ$ and 180° . A LAB distribution back-calculated from such a curve fit the experimental data except at wide positive LAB angles (see Fig. 5). The signal to noise ratio is particularly bad at these angles, but if the scattering is indeed less than that expected from the statistical complex

model at wide-angles, it could indicate that a LiSF_6 complex with a lifetime comparable to a rotational period is formed. Such "osculating complexes" have been observed previously.³⁵ If the reaction does proceed via formation of a strongly coupled complex, the products might be expected to recoil with a relatively low energy, similar to that estimated in Table I, because the total energy available to the products would be equipartitioned among the many degrees of freedom in the complex.



Quantitative comparisons of the $\text{M} + \text{CCl}_4$ product angular distributions shown in Fig. 9 could be misleading owing to the reported⁶ strong coupling of the E' and θ distributions for these reactions. However, the present results clearly indicate that the $\text{Li} + \text{CCl}_4$ reaction produces appreciably less product scattering into the forward CM hemisphere than do the corresponding K , Rb , and $\text{Cs} + \text{CCl}_4$ reactions. The total reaction cross section listed in Table III correlates well with the values of 150 , 100 and 60\AA^2 for Cs , Rb and $\text{K} + \text{CCl}_4$ respectively reported in Ref. 5 and the value for $\text{K} + \text{CCl}_4$ inferred from the attenuation of the elastic scattering in Ref. 33. Thus, the two trends, decrease in reaction yield and shift of preferred CM recoil angle to larger values as the mass of the alkali metal is decreased, that were observed in Ref. 5 hold for the $\text{Li} + \text{CCl}_4$ reaction studied here as well. These systems present another opportunity for theoretical calculations to elucidate evident trends.



The total reaction cross section reported for $\text{Li} + \text{CH}_3\text{I}$ in Table III is comparable to the value of 35\AA^2 reported for $\text{K} + \text{CH}_3\text{I}$ in Ref. 2b; the

total reaction cross section estimated from the attenuation of the elastic scattering of $K + CH_3I$ also falls in the same range ($25-47\text{\AA}^2$).³³ The behavior of $Na + CH_3I$ appears somewhat anomalous; a value of 5\AA^2 was reported in Ref. 3. The Na reaction is also the least exoergic of these three reactions and this fact may explain³⁶ its anomalously small total reaction cross section.

The LiI is scattered predominately backward in the CM system in agreement with the previously reported behaviors for the Cs and Rb^{2c}, K^{2b}, and Na³ reactions with CH_3I . However, the present results leave little doubt that the LiI-CM product angular distribution is considerably broader than that of the corresponding NaI and KI. The high translational product recoil energy of LiI is also in approximate accord with the values found for NaI and KI; FVA results are not available for the Cs and Rb reactions. There are extensive trajectory calculations on several potential surfaces for the $M + CH_3I$ reactions;³² these calculations predict the observed backward scattering of the products, but fail to reproduce the high product translational energies observed, presumably because the surfaces do not have enough repulsive character between the products. Further calculations on improved surfaces would be desirable to determine if the broader LiI-CM angular distribution observed here is due to the effect of the small mass of Li on the reaction dynamics. Such an effect was suggested in Part I as the reason that the LiZ product distributions from reactions of Li with diatomic halogens were broader than the corresponding distributions due to the heavier alkali metals.

ACKNOWLEDGEMENT

We are indebted to Mr. S.-M. Lin, L. C.-H. Loh, and C.A. Mims for help in the collection and analysis of some of the data and for many informative discussions. This work was supported by the Atomic Energy Commission.

REFERENCES

1. D.D. Parrish and R.R. Herm, *J. Chem. Phys.* 51, 5467 (1969); this article is referred to in the text as Part I.
2. (a) D.R. Herschbach, *Disc. Faraday Soc.* 33, 144 (1962); (b) G.H. Kwei, J.A. Norris, and D.R. Herschbach, *J. Chem. Phys.* 52, 1317 (1970); (c) G.H. Kwei, Ph.D. thesis, University of California, Berkeley, 1967.
3. J.H. Birely, E.A. Entemann, R.R. Herm, and K.R. Wilson, *J. Chem. Phys.* 51, 5461 (1969).
4. T.H. Bull and P.B. Moon, *Disc. Faraday Soc.* 17, 54 (1954).
5. K.R. Wilson and D.R. Herschbach, *J. Chem. Phys.* 49, 2676 (1968).
6. S. Riley, P.E. Siska, and D.R. Herschbach, to be published.
7. S.M. Freund, G.A. Fisk, D.R. Herschbach, and W. Klemperer, *J. Chem. Phys.* (to be published).
8. R.R. Herm and D.R. Herschbach, *J. Chem. Phys.* 52, 5783 (1970).
9. Values between 45 and 90 kcal/mole have been reported for the electron affinity of NO_2 . Reference 8 gives a complete discussion.
10. D.D. Parrish, Ph.D. thesis, University of California, Berkeley, 1970.
11. J.H. Birely, R.R. Herm, K.R. Wilson and D.R. Herschbach, *J. Chem. Phys.* 47, 993 (1967).
12. For reviews, see: E.F. Greene, A.L. Moursund, and J. Ross, *Adv. Chem. Phys.* 10, 135 (1966); E.F. Greene and J. Ross, *Science* 159, 587 (1968).
13. D.O. Ham and J.L. Kinsey, *J. Chem. Phys.* 53, 285 (1970).
14. S. Datz, D.R. Herschbach, and E.H. Taylor, *J. Chem. Phys.* 35, 1549 (1961).
15. (a) E.A. Entemann, Ph.D. thesis, Harvard University, Cambridge, Massachusetts, 1967; (b) E.A. Entemann and D.R. Herschbach, *Disc. Faraday Soc.* 44, 289 (1967).

16. The NO_2 pressure in the oven, as read on a thermocouple gauge, was 1.1 Torr; this would correspond to an equilibrium $\text{N}_2\text{O}_4/\text{NO}_2$ source pressure ratio of $\sim 1\%$. However, owing to the possible contamination of this thermocouple gauge by the corrosive gases employed in this study, it is desirable to get other estimates of the N_2O_4 concentration in the beam. In Part I the ICl beam was prepared by immersing ICl in an ice bath at 0°C ; thus, the ICl oven pressure was certainly no more than the equilibrium vapor pressure of ICl at 0°C , and was probably considerably lower, as a flow situation existed. Comparisons of the Li beam attenuations in the NO_2 and ICl experiments and of the Li- NO_2 and Li-ICl resolution corrected total cross sections provide an upper limit of 6.2 Torr for the NO_2 oven pressure. This indicates that the $\text{N}_2\text{O}_4/\text{NO}_2$ ratio had to be less than 6% in the oven, and actually was probably considerably less. Perhaps the best argument against any measurable role of N_2O_4 in this experiment is provided by a previous crossed beam study (Ref. 8) of $\text{Cs} + \text{NO}_2$; using a combination of magnetic and electric deflection analysis, Ref. 8 reported appreciable CsO signal, but no CsNO_2 signal. Since the gas oven design employed here was identical to that used in Ref. 8 and both experiments were certainly run with very similar NO_2 pressures, this observation indicates a negligible N_2O_4 concentration in the NO_2 beam employed here.
17. R.A. Berg, L. Wharton, W. Klemperer, A. Buchler, and J.L. Stauffer, *J. Chem. Phys.* 43, 2416 (1965).
18. G. Herzberg, Molecular Spectra and Molecular Structure I. Spectra of Diatomic Molecules (D. van Nostrand Co. Inc., Princeton, N.J., 1950).

19. (a) R.R. Herm and D.R. Herschbach, *J. Chem. Phys.* 43, 2139 (1965);
(b) C. Maltz and D.R. Herschbach, *Disc. Faraday Soc.* 44, 176 (1967);
(c) C. Maltz, Ph.D. thesis, Harvard University, Cambridge, Massachusetts, 1969.
20. M. Krauss, Compendium of ab initio Calculations of Molecular Energies and Properties (NBS Technical Note 438, United States Department of Commerce, Washington, D.C., 1967).
21. B. Bederson and E.J. Robinson, *Adv. Chem. Phys.* 10, 1 (1966).
22. J.E. Boggs, *J. Phys. Chem.* 68, 2379 (1964).
23. Landolt-Bernstein Zahlenwerte und Functionen, A.M. Hellwege and K.H. Hellwege, Eds. (Springer-Verlag, Berlin), Vol. 1, Part 3 (1951), pp. 510 ff.
24. C.H. Townes and A.L. Schawlow, Microwave Spectroscopy (McGraw-Hill, New York, 1955).
25. See, for example, D.R. Herschbach, *Adv. Chem. Phys.* 10, 319 (1966).
26. See the surfaces used in the Monte Carlo investigations of the alkali atom-halogen molecule reactions: N.C. Blais, *J. Chem. Phys.* 49, 9 (1968); M. Godfrey and M. Karplus, *J. Chem. Phys.* 49, 3602, (1968); P.J. Kuntz, E.M. Nemeth, and J.C. Polanyi, *J. Chem. Phys.* 50, 4607 (1969); and P.J. Kuntz, M.H. Mok, and J.C. Polanyi, *J. Chem. Phys.* 50, 4623 (1969).
27. S.J. Nalley, J.A.D. Stockdale, and R.N. Compton, *Bull. Am. Phys. Soc.* 15, 418 (1970).
28. R.E. Minturn, S. Datz, and R.L. Becker, *J. Chem. Phys.* 44, 1149 (1966).
29. R.S. Berry, *Chem. Rev.* 69, 533 (1969).
30. R. Grice, M.R. Cosandey, and D.R. Herschbach, *Ber. Buns. Physik. Chem.* 72, 975 (1968).

31. T.L. Cottrell, The Strengths of Chemical Bonds (Butterworth Scientific Publications, London, 1958).
32. See, for a review, M. Karplus, "Structural Implications of Reaction Kinetics" in Linus Pauling Festschrift (W.H. Freeman and Co., San Francisco, 1967).
33. J.A. Airey, E.F. Greene, G.P. Reck, and J. Ross, J. Chem. Phys. 46, 3295 (1967).
34. W.B. Miller, S.A. Safron, and D.R. Herschbach, Disc. Faraday Soc. 44, 108 (1967).
35. G.A. Fisk, J.D. McDonald, and D.R. Herschbach, Disc. Faraday Soc. 44, 228 (1967).
36. D.D. Parrish and R.R. Herm, J. Chem. Phys. 53, 2431 (1970).

TABLE I. Estimates of Recoil Energies^a

Reaction	E	ΔD_0	E' Best	E' Range
$\text{Li} + \text{NO}_2 \rightarrow \text{LiO} + \text{NO}$	1.88	10±4	2.4	2-3
$\text{Li} + \text{CH}_3\text{NO}_2 \rightarrow \text{LiNO}_2 + \text{CH}_3$	1.94		10.4	9-11
$\text{Li} + \text{SF}_6 \rightarrow \text{LiF} + \text{SF}_5$	2.02	56±7	1.6	1-2
$\text{Li} + \text{CCl}_4 \rightarrow \text{LiCl} + \text{CCl}_3$	2.03	43±5	17	1-43
$\text{Li} + \text{CH}_3\text{I} \rightarrow \text{LiI} + \text{CH}_3$	1.99	30±2	15	12-20

^aAll energies are given in kcal/mole. The initial relative translational kinetic energy of the reactants corresponding to the most probable source velocities is denoted by E; E' is the product recoil energy estimated from the FVA transformation procedure; $\Delta D_0 = D_0(\text{LiX}) - D_0(\text{RX})$ is the reaction exoergicity. Bond dissociation energy data were taken from: for LiF, LiCl, and LiI, L. Brewer and E. Brackett, Chem. Rev. 61, 425 (1961); for LiO, Ref. 8; for NO₂ and CH₃I, G. Herzberg, Molecular Spectra and Molecular Structure III. Electronic Spectra and Electronic Structure of Polyatomic Molecules (D. Van Nostrand Co., Inc., Princeton, N.J., 1966); for SF₆, Ref. 7; for CCl₄, Ref. 31.

TABLE II. LiZ-CM Distribution Expansion in Legendre Polynomials^a

Reactant	a_0	a_1	a_2	a_3	a_4	a_5
NO ₂	0.499	0.279	0.114	0.086	0.006	0.016
CH ₃ NO ₂	0.721	0.246	0.031	0.023	-0.027	0.006
SF ₆	0.704	0.186	-0.087	0.131	0.012	0.054
CCl ₄	17.658	-7.239	-19.952	6.880	2.049	1.604
CH ₃ I	2.061	-0.627	-0.659	0.173	-0.027	0.079

^aThese coefficients are defined by $I_{LiZ}(\theta) = \sum_n a_n P_n(\cos \theta)$
and are normalized such that $\sum_n a_n = 1$.

TABLE III. Total and Reactive Cross Sections^a

System	$\langle E^{-1/3} \rangle^{-3}$	C	$Q_{t,abs}$	$Q_{t,abs}^{eff}$	$Q_R(A)$	$Q_R(B)$
Li + NO ₂	2.45	320	390	210	15	16
Li + CH ₃ NO ₂	2.53	740	550	280	58	55
Li + SF ₆	2.71	650	520	260	17	18
Li + CCl ₄	2.73	1110	650	320	37	43
Li + CH ₃ I	2.67	780	560	280	27	27

^aThe mean elastic collision energies, $\langle E^{-1/3} \rangle^{-3} = 1.36 (\mu/m_{Li})$
k T_{Li} are given in kcal/mole, the van der Waals force constants in 10⁻¹²
erg-Å⁶, and the cross sections in Å². The total cross sections were
calculated for relative velocities corresponding to $\langle E^{-1/3} \rangle^{-3}$.

FIGURE CAPTIONS

Fig. 1. Measured LAB angular distributions derived by magnetic deflection analysis and corrected for the viewing factor. The X's show the total scattered intensity ($I_{Li} + I_{LiZ}$); the circles show the derived Li intensity. The solid lines indicate the "smoothed" Li angular distributions.

Fig. 2. Plot of CM angular distributions (plotted as $I_{Li}(\theta)\sin\theta$) for the elastic scattering, derived by transforming the smooth solid curve fits to the LAB data for Li scattering shown in Fig. 1; data taken from the LAB curves at 5° intervals were transformed. The open circles were obtained from LAB data with $\theta > 0^\circ$, the dark circles from LAB data with $\theta < 0^\circ$. The data were linearly extrapolated to $\theta = 180^\circ$ (dotted lines). Data for the scattering of Li from cyclohexane not shown in Fig. 1 were also transformed; the derived CM angular distribution is shown as the dashed lines. The Li+cyclohexane data were normalized to the Li scattering produced by each of the reactive gases at narrow angles ($0 < \theta < 10^\circ$) by normalizing each curve to the small angle scattering form factor given in Eq. (16) of Part I.

Fig. 3. LAB angular distribution of LiO product from $Li + NO_2$ derived from data points shown in Fig. 1; the solid curve through the data points indicates the "best" distribution based on analysis of the errors in the data points. The error bars denote only those errors introduced by uncertainties in the calibration of the ability of the inhomogeneous electromagnet to deflect aside Li atoms (this source of error is discussed extensively in Part I). The dotted curve gives the calculated distribution in centroid angles for an energy independent collision cross section. The dashed curve is back-calculated from the derived CM product angular

distribution shown in Fig. 8 by averaging over thermal velocity distributions in both beams. Also shown is a kinematic diagram indicating the most probable reactant thermal source velocities, the corresponding centroid vector \underline{C} , and the relative velocity vector \underline{V} ; the circles indicate the lengths of the LiO recoil velocities for four of the possible product recoil energies, E' (kcal/mole). The two Li temperatures refer respectively to runs without and with the deflecting magnet (see Part I) and indicate the range of uncertainty in the Li temperature.

Fig. 4. Calculated centroid distribution, kinematic diagram, and LAB angular distribution of LiNO_2 from $\text{Li} + \text{CH}_3\text{NO}_2$, derived from the data of Fig. 1. The solid curve indicates the "best fit" to the data; the dashed curve was back-calculated from the CM angular distribution shown in Fig. 9.

Fig. 5. Calculated centroid distribution, kinematic diagram, and LAB angular distribution of LiF from $\text{Li} + \text{SF}_6$, derived from data of Fig. 1. The solid curve indicates the "best fit" to the data. The other two curves (dash and dash-dot-dash which coincide for $\theta \leq 70^\circ$) were back calculated from the LiF -CM angular distributions shown in Fig. 9 (solid and dash-dot-dash respectively).

Fig. 6. Calculated centroid distribution, kinematic diagram, and LAB LiCl angular distribution from $\text{Li} + \text{CCl}_4$, derived from the data of Fig. 1. The solid curve indicates the "best fit" to the data. The other two curves (dash and dash-dot-dash) were back-calculated from the LiCl -CM angular distributions shown in Fig. 9 (solid and dash-dot-dash respectively); these latter two curves coincide for $\theta \leq 100^\circ$.

Fig. 7. Calculated centroid distribution, kinematic diagram, and LAB LiI angular distribution from $\text{Li} + \text{CH}_3\text{I}$, derived from the data of Fig. 1. The solid curve indicates the "best fit" to the data. The other two curves

(dash and dash plus dash-dot-dash) were back-calculated from the LiI-CM distributions shown in Fig. 9 (solid and solid plus dash-dot-dash curves respectively).

Fig. 8. Comparison of CM product angular distributions. The LiO product angular distribution from $\text{Li} + \text{NO}_2$ was obtained by transforming the solid curve of Fig. 3 at 5° intervals by the FVA procedure; the open circles give data for positive CM angles (rotations of the recoil velocity vector counter-clockwise from the original Li direction); the dark circles refer to negative values of θ ; the data were extrapolated to $\theta = 180^\circ$ from the last open circle data point. The K, Rb, and Cs + Cl_2 data were taken from R. Grice and P.B. Emedocles, J. Chem. Phys. 48, 5352 (1968). The LiX angular distributions reported in Part I for $\text{Li} + \text{Cl}_2$, Br_2 and ICl all lie within the shaded region denoted $\text{Li} + \text{XY}$. All distributions were normalized to unity at $\theta = 0^\circ$.

Fig. 9. Comparisons of CM product angular distributions; all distributions normalized to unit peak height. The Li data were obtained from Figs. 4-7; the transformation procedure was the same as for Fig. 8. The K, Rb, and Cs + CCl_4 curves were taken from Ref. 5; the Na + CH_3I curve from Ref. 3; and the K + CH_3I curve from Ref. 2b. For $\text{Li} + \text{CCl}_4$ and CH_3I , back-calculations (for comparison with the original LAB distributions) were performed for both the derived CM distributions (solid curves) and for distributions assumed to be level from the peak in the derived distributions out to $\theta = 180^\circ$ (dash-dot-dash curves).

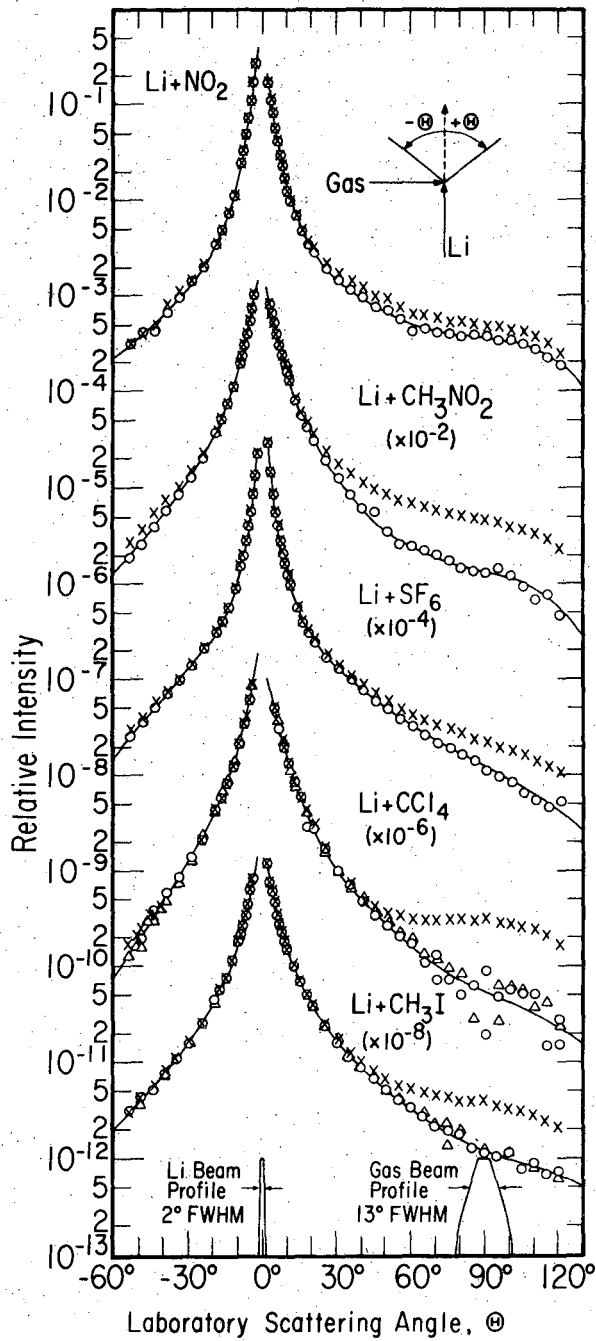
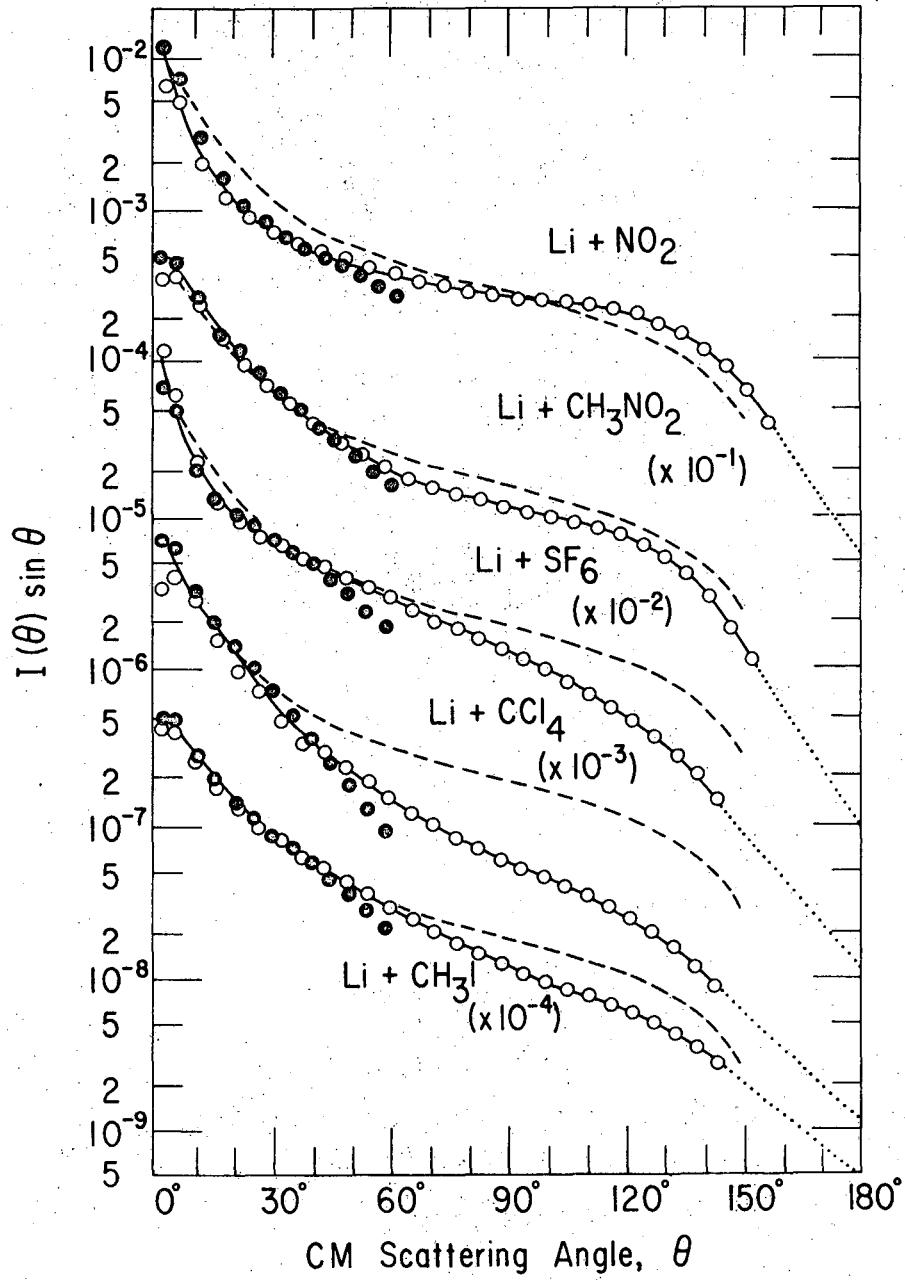
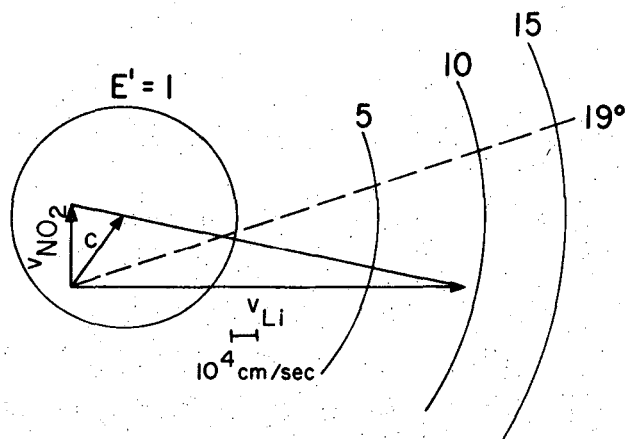
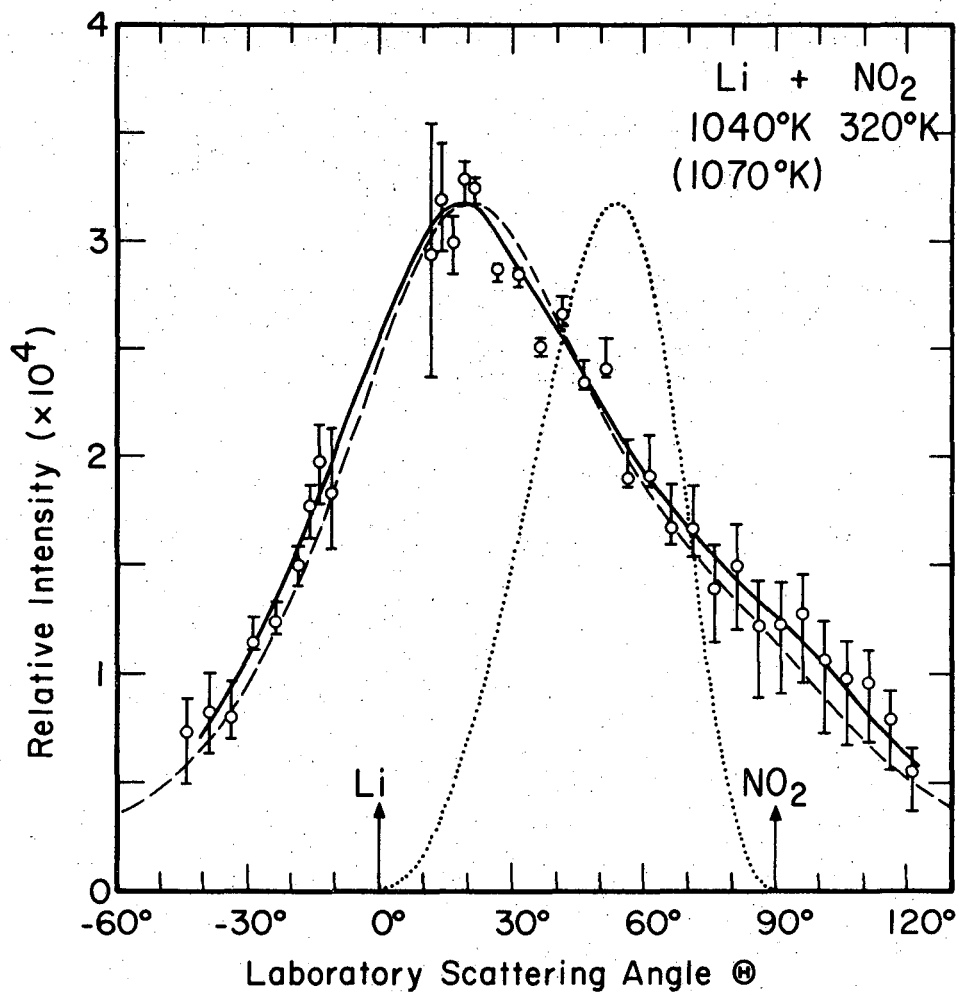


Fig. 1.



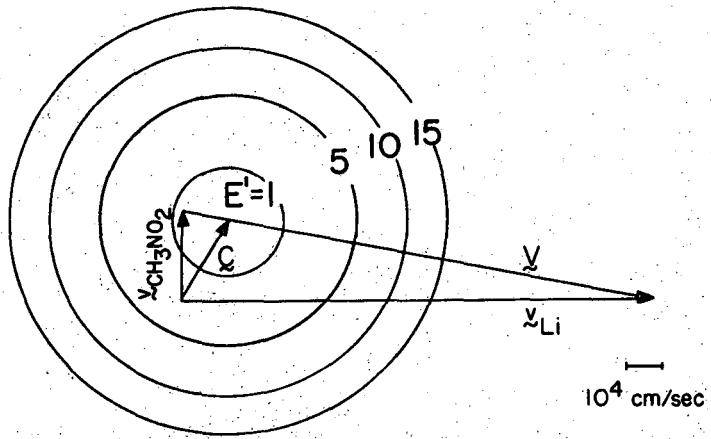
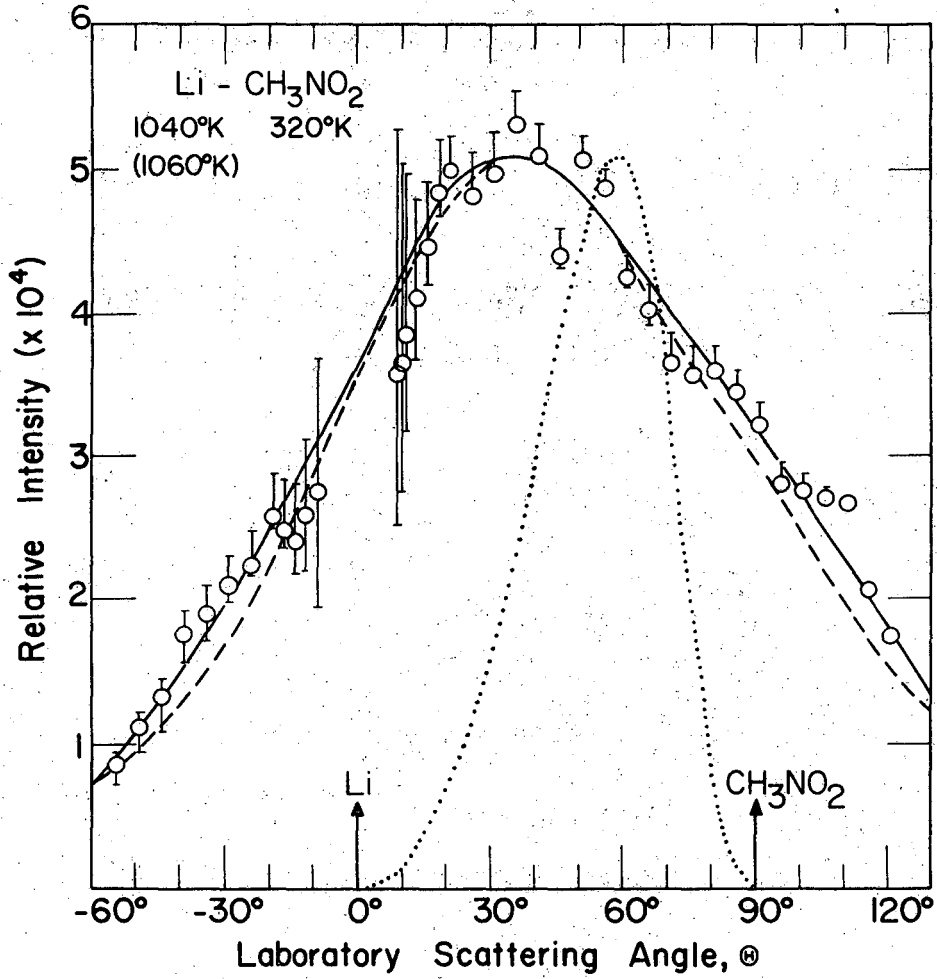
XBL 6910-5925

Fig. 2.



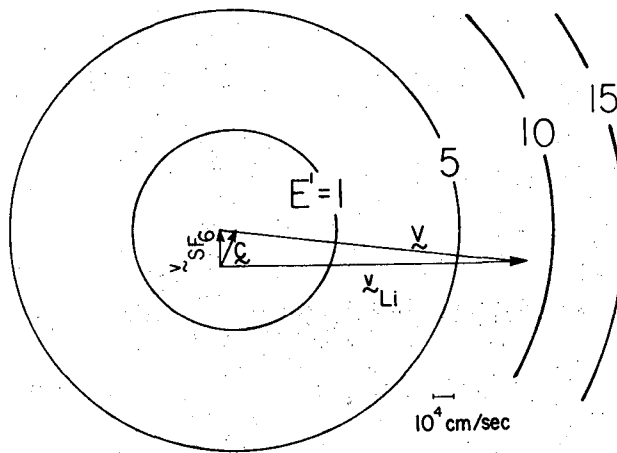
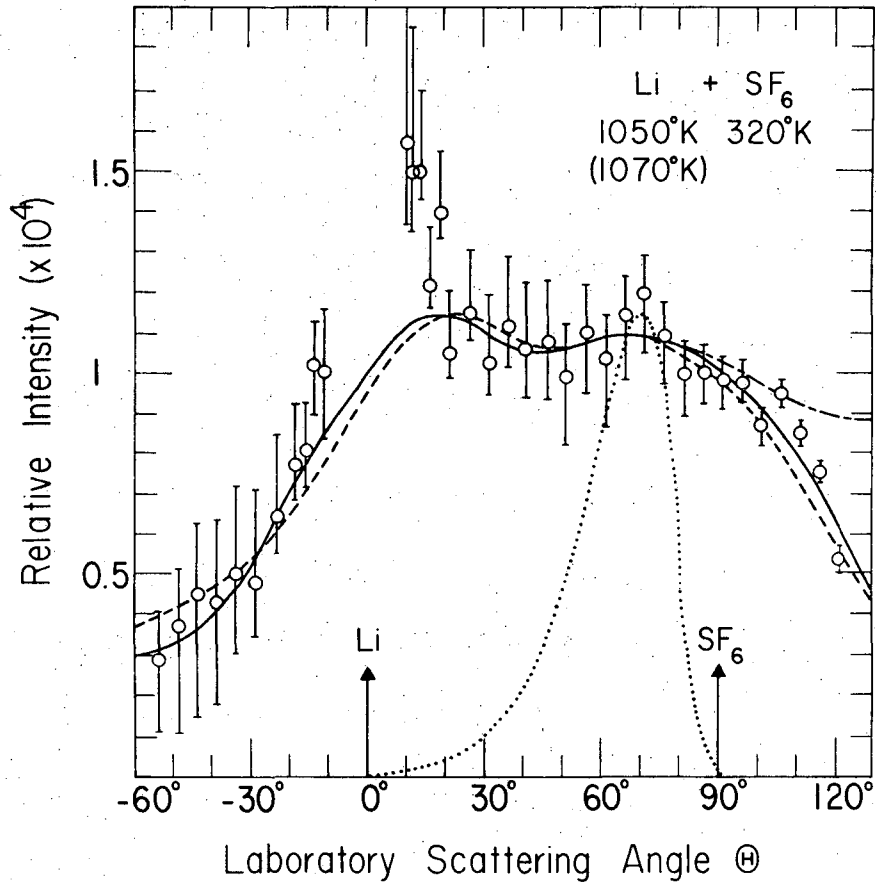
261 6811 6196

Fig. 3.



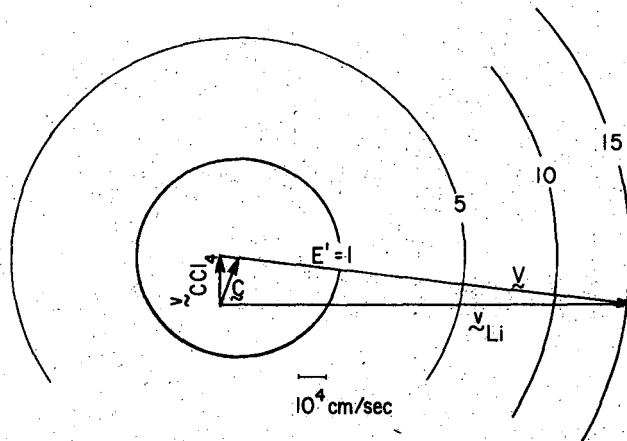
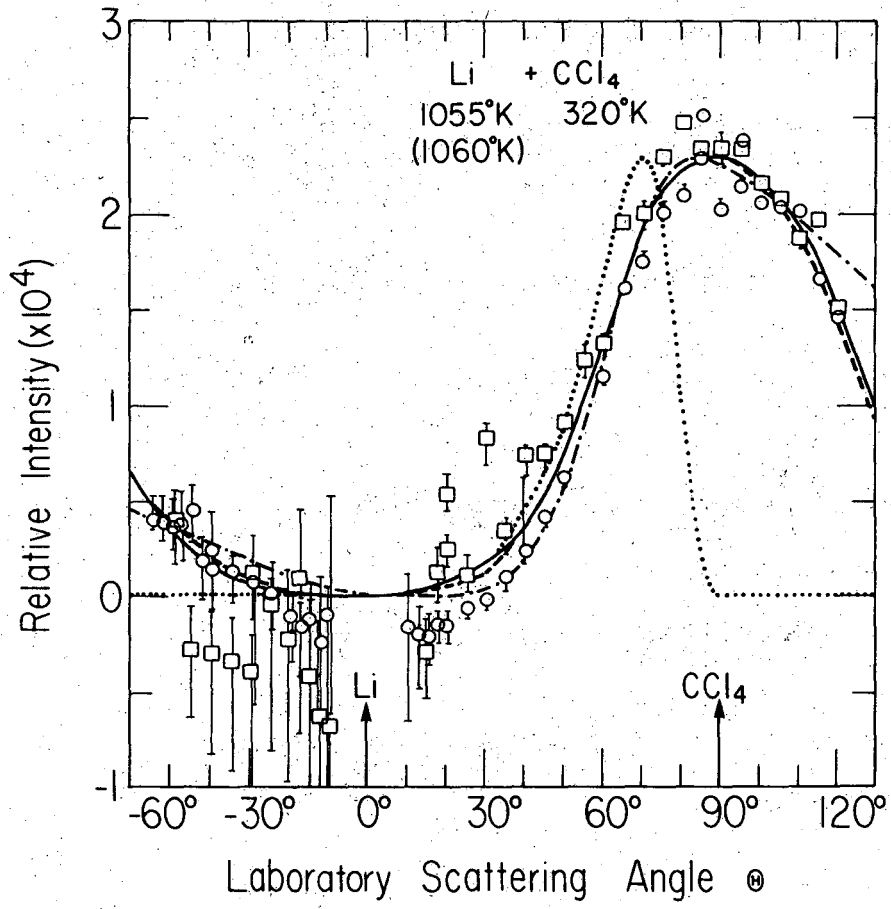
XBL 694-417

Fig. 4.



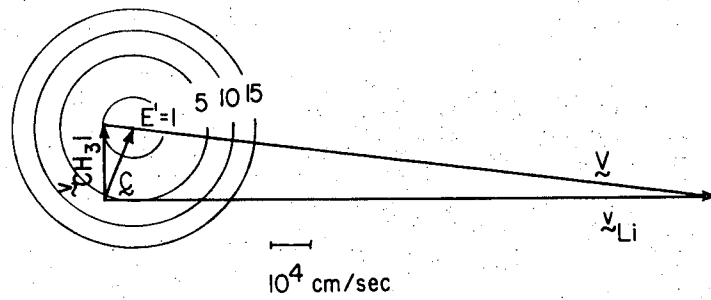
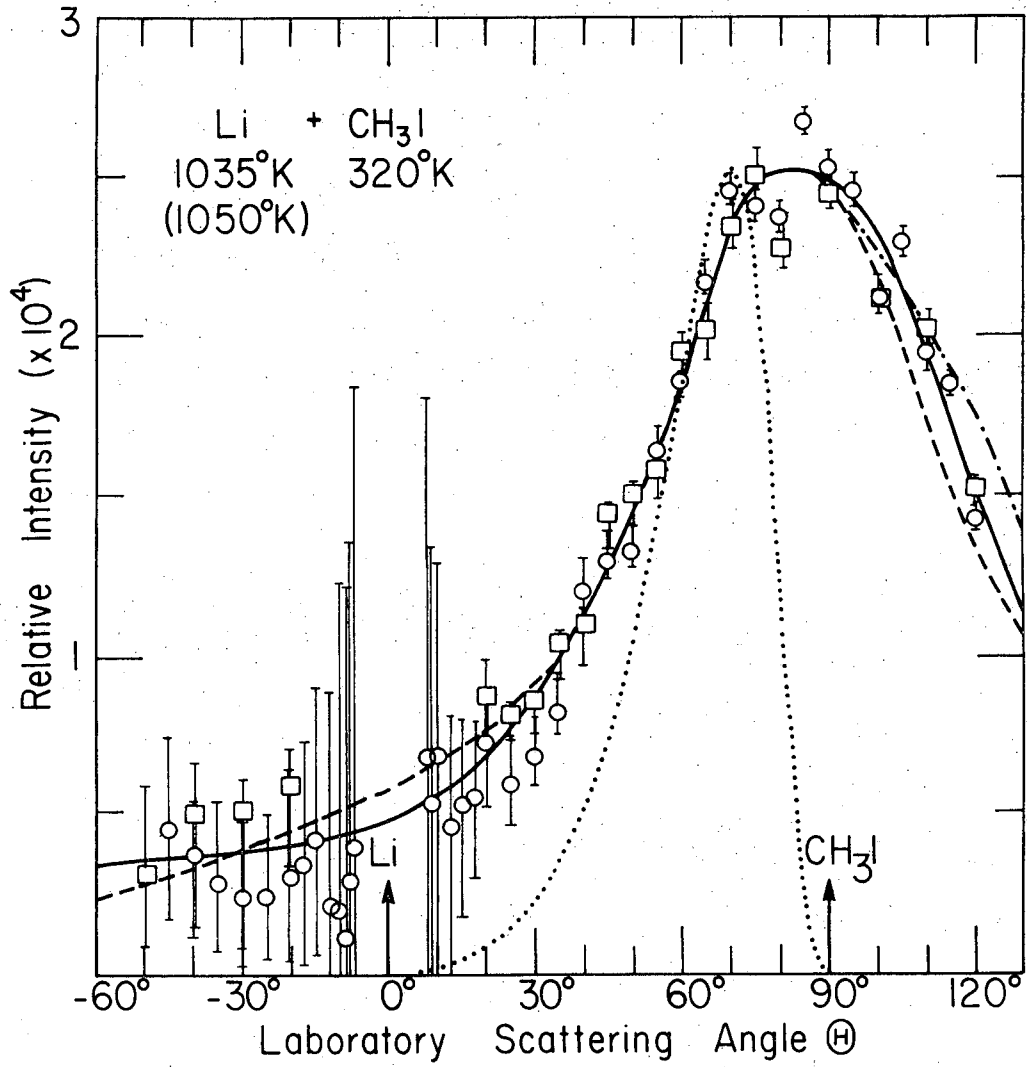
XBL 6910-5927

Fig. 5.



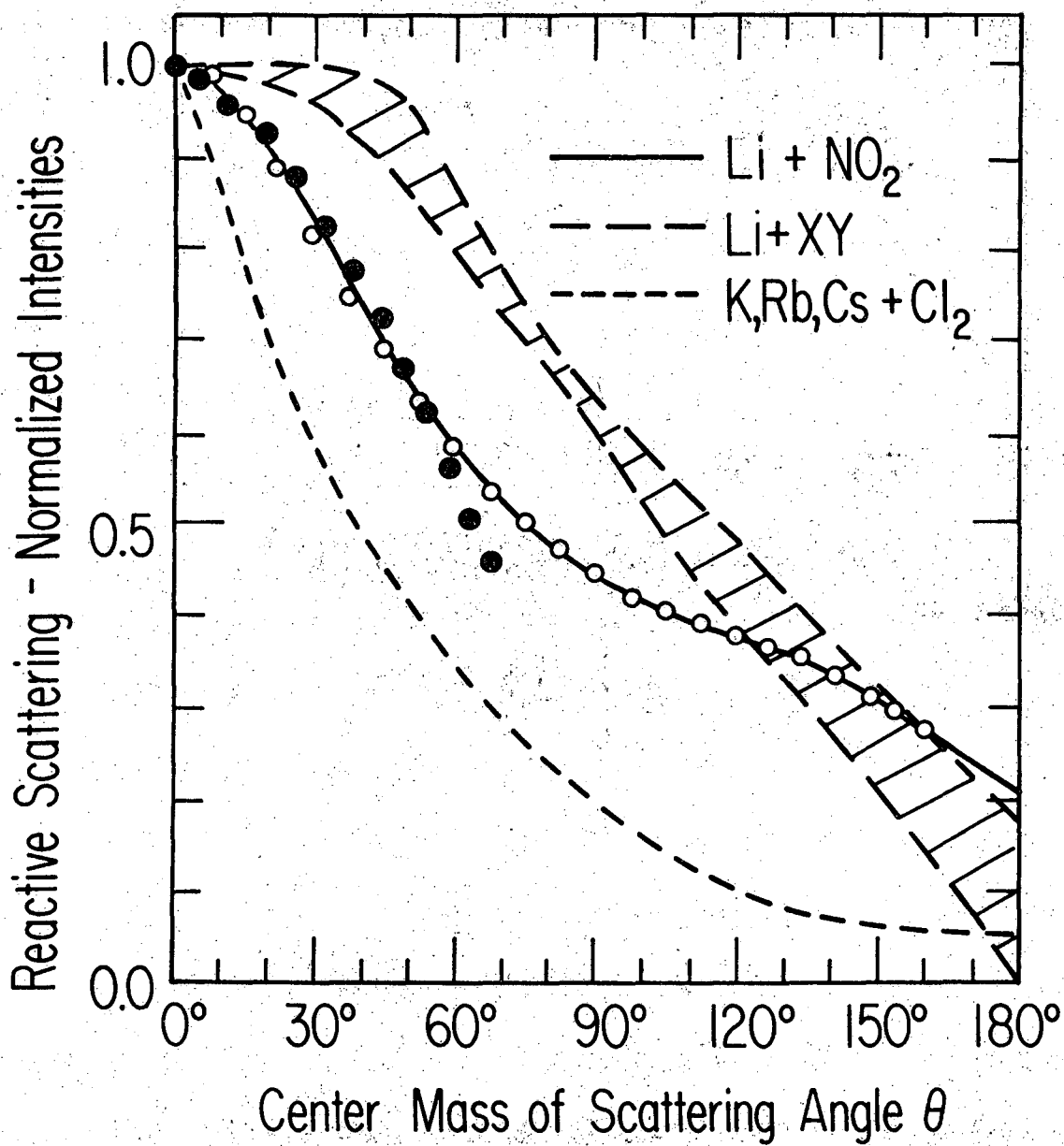
XBL 6910-5926

Fig. C.



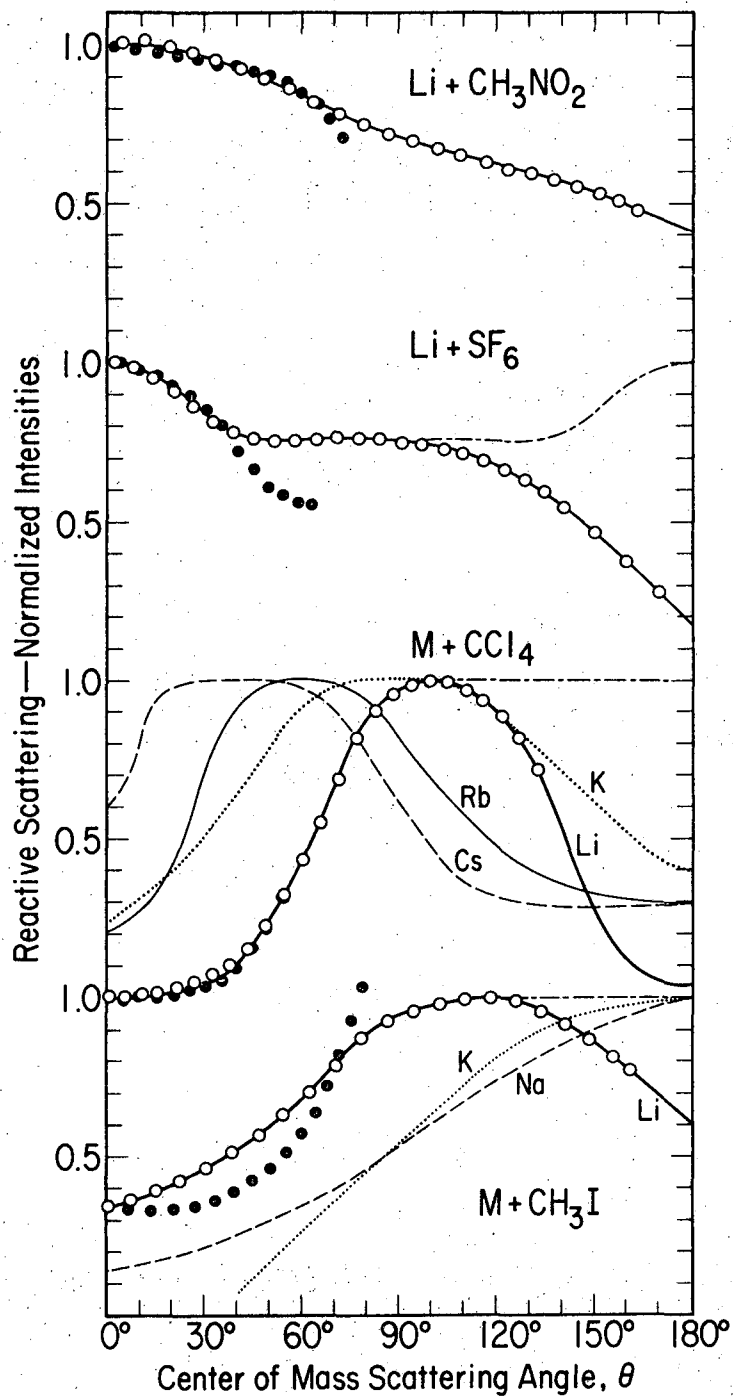
XBL 6910-5928

Fig. 7.



XBL 6910-5929

Fig. 8.



XBL 6910-5930

Fig. 9.

LEGAL NOTICE

This report was prepared as an account of Government sponsored work. Neither the United States, nor the Commission, nor any person acting on behalf of the Commission:

- A. Makes any warranty or representation, expressed or implied, with respect to the accuracy, completeness, or usefulness of the information contained in this report, or that the use of any information, apparatus, method, or process disclosed in this report may not infringe privately owned rights; or*
- B. Assumes any liabilities with respect to the use of, or for damages resulting from the use of any information, apparatus, method, or process disclosed in this report.*

As used in the above, "person acting on behalf of the Commission" includes any employee or contractor of the Commission, or employee of such contractor, to the extent that such employee or contractor of the Commission, or employee of such contractor prepares, disseminates, or provides access to, any information pursuant to his employment or contract with the Commission, or his employment with such contractor.

TECHNICAL INFORMATION DIVISION
LAWRENCE RADIATION LABORATORY
UNIVERSITY OF CALIFORNIA
BERKELEY, CALIFORNIA 94720